Partially crystallized $La_{0.5}Sr_{0.5}MnO_3$ thin films by laser ablation and their enhanced low-field magnetoresistance

J.-M. Liu[a)]
Laboratory of Solid State Microstructures, Nanjing University, Nanjing 210093, People's Republic of China; Institute of Materials Research and Engineering, Singapore 117602; and Center for Superconducting and Magnetic Materials, National University of Singapore, Singapore

J. Li, Q. Huang, L. P. You, S. J. Wang, and C. K. Ong
Center for Superconducting and Magnetic Materials and Department of Physics, National University of Singapore, Singapore

Z. C. Wu, Z. G. Liu, and Y. W. Du
Laboratory of Solid State Microstructures, Nanjing University, Nanjing 210093, People's Republic of China

(Received 20 September 1999; accepted for publication 28 February 2000)

Amorphous, partial-crystallized, and epitaxial $La_{0.5}Sr_{0.5}MnO_3$ thin films have been deposited at various temperatures of 200–650 °C on (001) $SrTiO_3$ substrates using pulsed-laser deposition. The x-ray diffraction and high-resolution transmission electron microscopy indicate complete (001) orientation of the crystalline structures in these films. Enhanced low-field magnetoresistance effect has been observed for the partial-crystallized thin films where the nanosized ferromagnetic crystals are embedded in nonferromagnetic amorphous matrix. It is argued that the amorphous layer separating the neighboring nanocrystals behaves as the barrier for the spin-polarized tunneling and/or spin-dependent scattering, resulting in enhanced magnetoresistance at low magnetic field. © *2000 American Institute of Physics.* [S0003-6951(00)05316-X]

Special research attention has recently been paid to manganese perovskite oxides $La_{1-x}A_xMnO_{3-y}$ (A=divalent cation such as Ca, Sr, Ba), due to the fact that these oxides exhibit colossal magnetoresistance (MR) effect.[1,2] It has been reported that the thin film samples show an MR ratio (MR $=[\rho(0)-\rho(H)]/\rho(0)$, where ρ is sample resistivity and H is applied magnetic field) of over 90% at a high magnetic filed ($H=\sim 15$ T). However, the low-field MR ratio remains quite small. Typically, a MR ratio of just a few percent (2%–3%) was reported for epitaxial $La_{1-x}Ca_xMnO_3$(LCMO) or $La_{1-x}Sr_xMnO_3$(LSMO) thin films at a magnetic field of a few kOe.[2] Researchers have made an effort to exploit the microstructure in order to enhance the low-field MR.[3] It has been found that polycrystalline LCMO or LSMO thin films of fine grain size and artificial defects or boundaries exhibit much higher low-field MR ratio than that of epitaxial samples, at least at low temperature T.[4]

The MR effect in manganese oxides is explained in terms of the double-exchange model. The corresponding transition points, T_c (for ferromagnetic) and T_m (for insulating-metallic), respectively, are very close to each other. In the polycrystalline samples, the enhanced MR ratio below T_c is ascribed to the interfaces and grain boundaries where the ferromagnetic spin alignment shows disordered status to some extent. The underlying physical mechanism is the spin-polarized tunneling (SPT)[5–9] or spin-dependent scattering (SDS)[3] across these interfaces or boundaries.

It is therefore popular for experimentalists to explore new technique for embedding various spin-disordered media into the microstructures in order to enhance the low-field MR as largely as possible.[4,9–16] In this letter, we report our experiment on partially crystallized LSMO($x=0.5$) thin films where nanosized LSMO crystals are embedded in amorphous homogeneous matrix. The reason we choose LSMO ($x=0.5$, same below) is that LSMO is not a pure ferromagnet. It is not far from the ferromagnet/charge-ordering (CO) boundary at low T.[17] LSMO is not a typical system as LCMO where CO is often observed at low T. Up to date, there is rare direct evidence such as transmission electron microscopy or electron diffraction available to identify CO state in LSMO.

The LSMO thin films were deposited on (001)-oriented $SrTiO_3$ wafers using pulsed-laser deposition (PLD). The PLD experiment was performed utilizing KrF excimer laser of wavelength of 248 nm, pulse width of 30 ns.[18] The optimized laser fluency of 1.7 J/cm^2 and reprate of 5 Hz were used during the ablation, while the oxygen ambient pressure remained constant at 0.25 mbar. The films of 800 nm in thickness and 10×1.0 mm^2 in in-plane dimension were deposited and then cooled down to room temperature. The crystallization status of the samples was controlled by adjusting deposition temperature T_s, ranging from 200 to 650 °C, and then checked with x-ray diffraction (XRD) and high-resolution transmission electron microscopy (HRTEM). The Oxford superconducting vibrating sample magnetometer (VSM) was used to characterize the magnetic property of the samples. The electro- and magneto-transport properties were measured by the standard four-probe method with data collected by a personal computer. The ac magnetic field of $\pm$ 4 kOe in magnitude and 0.01 Hz in frequency was applied in parallel to the sample surface while the data were taken.

Figure 1 presents the XRD θ–2θ spectra around LSMO-(002) reflection for a series of samples deposited at various

a)Electronic mail: liujm@nju.edu.cn

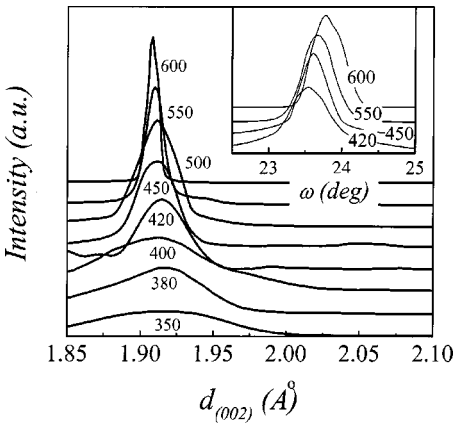

FIG. 1. XRD θ–2θ spectra of the (002) reflection for the LSMO thin films deposited on (001) $SrTiO_3$ substrates at various temperatures as indicated. The inset gives the ω scans with respect to the (002) reflection.

T_s as indicated. The samples deposited When $T_s = 200\,^{\circ}\mathrm{C}$, the samples were completely amorphous. Epitaxial structure is obtained once $T_s = 600\,^{\circ}\mathrm{C}$ and over. at $T_s < 400\,^{\circ}\mathrm{C}$ show diffusive diffraction peak around $d = 1.90$–$1.93\,\text{Å}$, and thus they are amorphous. As $T_s > 400\,^{\circ}\mathrm{C}$, the peak becomes sharper. At $T_s = 600\,^{\circ}\mathrm{C}$, the (002) peak is already very sharp. The crystalline phase appears in the samples for $T_s > 400\,^{\circ}\mathrm{C}$, as confirmed by our HRTEM observation below. In addition, a slight shift of the peak toward small d side is observed as T_s increases. This predicts that the lattice parameters decrease as the sample evolves from amorphous state to completely crystallized one. A rocking curve measurement produces a well-defined peak with respect to (002) reflection as long as T_s is higher than 400 °C. The obtained data are presented as the inset in Fig. 1. We therefore conclude that the crystalline phase in the partially crystallized samples keeps (001) orientation or is even epitaxial, whereas the thin films deposited at $T_s > 550\,^{\circ}\mathrm{C}$ are epitaxially grown.

The electrical resistivity and MR response of these samples as a function of T were measured. We first look at the MR response to H. As an example, the data at $T = 77\,\mathrm{K}$ for the partially crystallized sample deposited at $T_s = 450\,^{\circ}\mathrm{C}$ are presented in Fig. 2. This sample exhibits the highest MR ratio (expressed in ρ/ρ_0 here). The nonlinear $\rho/\rho_0 \sim H$ response remains very similar to that for polycrystalline sample where SPT and/or SDS are responsible for the

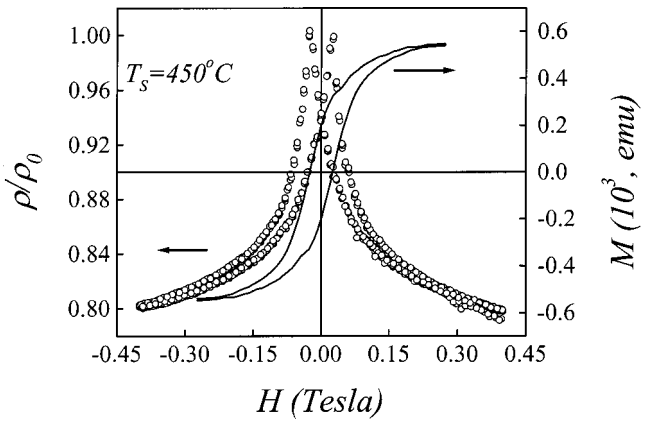

FIG. 2. The ρ/ρ_0–H and M–H hysteresis at $T = 77$ K as a function of time for the LSMO film deposited at 450 °C.

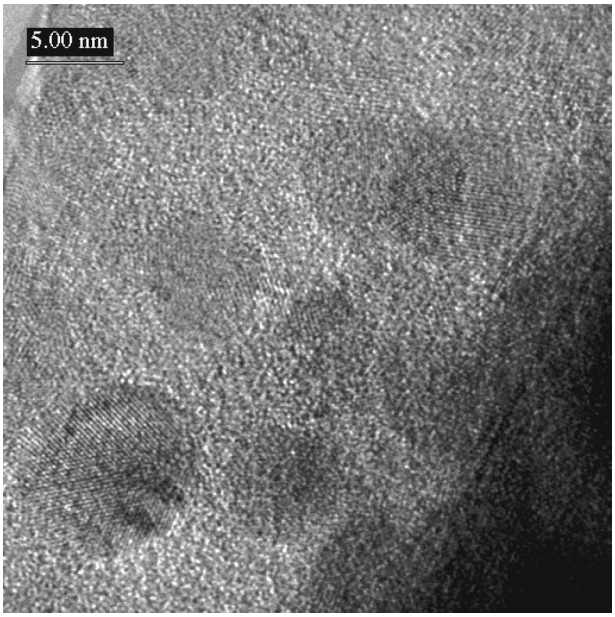

FIG. 3. HRTEM image of the LSMO film deposited at 450 °C.

nonlinearity.[3,4,6–8] These results provide us evidence that the underlying mechanism responsible for the MR effect may be the spin-dependent sequence like SPT and/or SDS. The amorphous phase separating the crystalline counterpart in the sample may play a role similar to the spin-disordered interface or boundaries.

The above argument gets support from the HRTEM imaging of the sample, as shown in Fig. 3. A number of crystalline particles of 5–10 nm in diameter embedded in the amorphous matrix are detected. The volume density of the particle number is around $10^{19}\,\mathrm{cm}^{-3}$. The lattice distance as derived from the image fringes of these particles is about 3.8–3.9 Å, very close to 3.82 Å, the lattice parameter of LSMO. On the other hand, the HRTEM images for the samples deposited at $T_s < 400\,^{\circ}\mathrm{C}$ show no contrast and the electron diffraction gives diffusive ring-like pattern, indicating that the microstructure is amorphous.

The VSM measurement reveals difference in magnetic property among the amorphous, partially crystallized, and crystalline samples. The magnetization M recorded at $H = 8$ kOe for three samples prepared separately at $T_s = 380$,

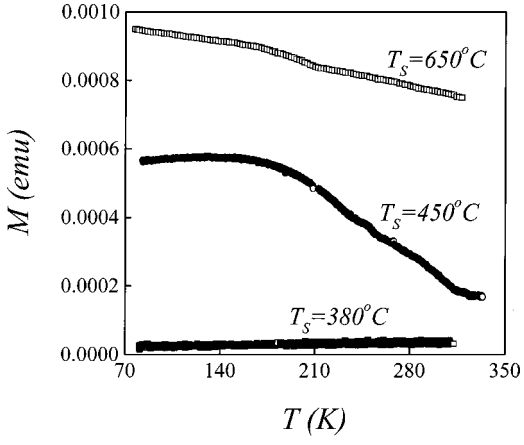

FIG. 4. Magnetization M at $H = 8$ kOe as a function of temperature for three samples deposited at 650, 450, and 380 °C, respectively.

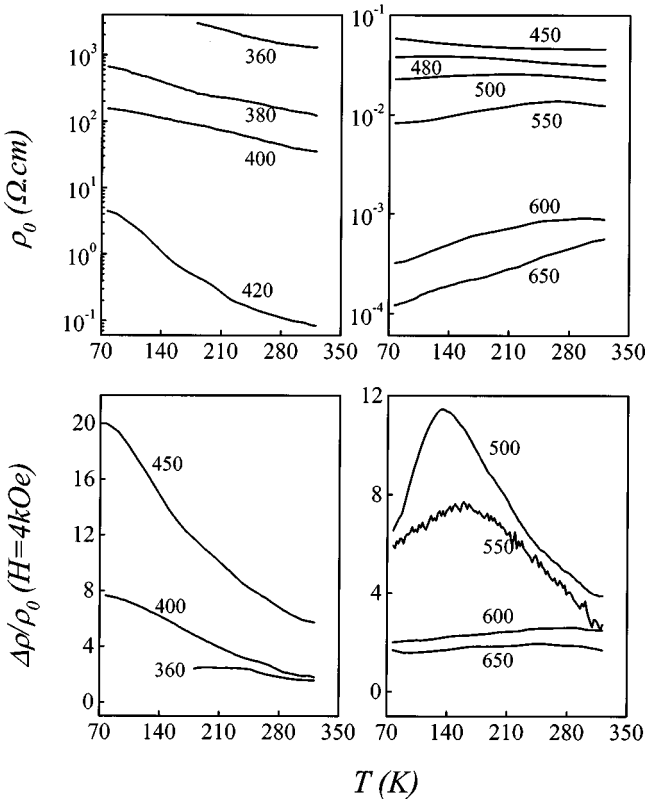

FIG. 5. Zero-field resistivity ρ_0 and magnetoresistance ratio $\Delta\rho/\rho_0$ at $H=4$ kOe as functions of temperature for a series of samples deposited at various temperatures as indicated.

450, and 650 °C is plotted as a function of T in Fig. 4. The sample for $T_s=380$ °C is nonferromagnetic over all T range. For the sample at $T_s=650$ °C, T_c is over room temperature. The ferromagnetic state at low T for the sample at $T_s=450$ °C is identified, giving $T_c\sim250$ K. Its magnetization is just a half of that for the 650 °C sample. We are therefore allowed to conclude that the partially crystallized sample still remains ferromagnetic at low T.

The above experiment gives us a physical picture for the enhanced low-field MR phenomenon at low T for the partially crystallized LSMO thin films, although further confirmation of this picture is required. The ferromagnetic nanosized LSMO crystals are embedded in the nonferromagnetic amorphous matrix. Under external field, SPT and/or SDS across the amorphous layer contribute to the enhanced low-field MR at low T. Along with this line, the electrical and magnetoresistance behaviors as function of T as presented below can be well understood. For a series of samples, the measured data are plotted in top panel of Fig. 5 for ρ and the bottom panel for MR ratio. The resistivity of the samples shows a change over eight orders of magnitude at low T and six orders of magnitude at high T as T_s changes from 360 to 650 °C. The amorphous LSMO exhibits typical insulating behavior over the whole T range. The resistivity data at $T<150$ K for the sample deposited at $T_s=360$ °C are too high to measure. The samples grown at $T_s<450$ °C remain insulating although the magnitude of ρ decreases with increasing T_s. At $T_s=450$ °C, the low T data show a signature of insulator-metal transition. The measured values of T_m for the samples prepared at $T_s=480$, 500, 550, and 600 °C are about 140, 200, 260, and 300 K, respectively. The sample deposited at $T_s=650$ °C remains metallic over all T range covered here. There is no CO feature observed for these samples. Keeping in mind that the amorphous structure is insulator and the crystalline one remains metallic, these effects can be well understood in the framework described above.

The magneto-transport behaviors for those samples are very different from one to another too. Both the amorphous and epitaxial thin films show very small low-field MR ratio, typically 2%–3% at $H=4$ kOe. The MR ratio at low T (e.g., 77 K) shows rapid growth with increasing T_s, reaching 8% at $T_s=400$ °C and even 20% at $T_s=450$ °C. As T_s increases further, the MR ratio falls again. At the same time, the MR ratio as a function of T exhibits a peak at certain position, say, 130 K as $T_s=500$ °C and 160 K as $T_s=550$ °C. The peak position is, however, much lower than T_c and T_m. The peaked MR ratio falls down to ~12% and 8%, respectively. Only 3% MR ratio is recorded for the sample prepared at $T_s=600$ °C. It is thus demonstrated that the partially crystallized LSMO shows significantly enhanced low-field MR ratio, especially at low T. The partially crystallized samples prepared at $T_s=450$ °C exhibit the optimal microstructure for the low-field MR enhancement. With well-controlled number density and spatial distribution of the crystalline LSMO particles in the microstructure, the low-field MR ratio can possibly be further enhanced.

The authors would like to acknowledge the support from NSF and the Key Projects for Basic Research of China, and LSSMS of Nanjing University.

[1] S. Jin, T. H. Tiefel, M. McCormack, R. A. Fastnacht, R. Ramesh, and L. H. Chen, Science **264**, 413 (1994).
[2] C. N. R. Rao and B. Raveau, *Colossal Magnetoresistance, Charge Ordering and Related Properties of Mangnaese Oxides* (World Scientific, Singapore, 1998).
[3] X. W. Li, A. Gupta, G. Xiao, and G. Q. Gong, Appl. Phys. Lett. **71**, 1124 (1997).
[4] A. Gupta, in *Colossal Magnetoresistance, Charge Ordering and Related Properties of Manganese Oxides*, edited by C. N. R. Rao and B. Raveau (World Scientific, Singapore, 1998), p. 189.
[5] H. Y. Hwang, S. W. Cheong, P. G. Radaelli, M. Marezio, and B. Batlogg, Phys. Rev. Lett. **75**, 914 (1995).
[6] R. Shreekala, M. Rajeswari, K. Ghosh, A. Goyal, J. Y. Gu, C. Kwon, Z. Trajanovic, T. Boettcher, R. L. Greene, R. Ramesh, and T. Venkatesan, Appl. Phys. Lett. **71**, 282 (1997).
[7] P. Raychaudhuri, T. K. Nath, A. K. Nigam, and R. Pinto, J. Appl. Phys. **84**, 2048 (1998).
[8] P. Raychaudhuri, K. Sheshadri, P. Taneja, S. Bandyopadhyay, P. Ayyub, A. K. Nigam, and R. Pinto, Phys. Rev. B **59**, 13919 (1999).
[9] S. Lee, H. Y. Hwang, B. I. Shraiman, W. D. Ratcliff, and S. W. Cheong, Phys. Rev. Lett. **82**, 4508 (1999).
[10] A. de Andres, M. Garcia-Hernandez, J. L. Martinez and C. Prieto, Appl. Phys. Lett. **74**, 3884 (1999).
[11] L. Balcells, J. Fontcuberta, B. Martinez, and X. Obradors, Phys. Rev. B **58**, R14697 (1998).
[12] H. Y. Hwang, S. W. Cheong, N. P. Ong, and B. Batlogg, Phys. Rev. Lett. **77**, 2041 (1996).
[13] X. L. Wang, S. X. Dou, H. K. Liu, M. Ionescu, and B. Zeimetz, Appl. Phys. Lett. **73**, 396 (1998).
[14] H. Y. Hwang, S. W. Cheong, P. G. Radaelli, M. Marezio, and B. Batlogg, Phys. Rev. Lett. **75**, 914 (1995).
[15] J. Fontcuberta, B. Martinez, A. Seffar, S. Pinol, J. L. Garcia-Munoz, and X. Obradors, Phys. Rev. Lett. **76**, 1122 (1996).
[16] Q. Huang, C. K. Ong, J. Li, and J.-M. Liu (unpublished).
[17] G. H. Jonker, Physica (Amsterdam) **22**, 707 (1956).
[18] J.-M. Liu and C. K. Ong, Appl. Phys. Lett. **73**, 1047 (1998).